

Systematic Effective Field Theory Analysis of the D=2+1 Quantum XY Model at Low Temperatures

Christoph P. Hofmann^a

^a Facultad de Ciencias, Universidad de Colima
Bernal Díaz del Castillo 340, Colima C.P. 28045, Mexico

October 31, 2018

Abstract

The low-temperature properties of the (2+1)-dimensional quantum XY model are studied within the framework of effective Lagrangians up to three-loop order. At zero temperature, the system is characterized by a spontaneously broken spin rotation symmetry, $O(2) \rightarrow 1$, where the corresponding Goldstone bosons are the spin waves or magnons. Even though there is no spontaneously broken order at finite T , the low-temperature behavior of the system is still governed by the spin waves. The partition function is evaluated and various thermodynamic quantities, including the order parameter, are derived in the presence of a weak external field. In particular, we show that the spin-wave interaction is repulsive at low temperatures, its magnitude depending on the strength of the external field. We compare our results with those for the (2+1)-dimensional antiferromagnetic Heisenberg model which, at $T = 0$, exhibits the spontaneously broken spin rotation symmetry $O(3) \rightarrow O(2)$.

1 Introduction

One of the most popular methods to address the low-temperature physics of systems exhibiting collective magnetic behavior is spin-wave theory. Ferromagnets and antiferromagnets have been analyzed extensively within this framework over the years, both in three and in two spatial dimensions. In particular, to cope with systems defined

in two spatial dimensions, modified spin-wave theory [1, 2] and spin-wave theory at constant order parameter [3] have been invented.

While spin-wave theory worked well for the Heisenberg model, it was rather unclear whether this method is also readily applicable to the quantum XY model. It was then shown in Refs. [4, 5] that this is indeed the case. Subsequent investigations based on spin-wave theory which address the quantum XY model in two spatial dimensions at zero temperature, can be found in Refs. [6–9].

In the present work, we are interested in the low-temperature regime of the $d=2+1$ quantum XY model, where the spin waves are the relevant degrees of freedom. Our approach, however, is based on an entirely different method – the method of effective Lagrangians which universally applies to any system whose low-energy properties are dominated by Goldstone bosons. Indeed, at zero temperature, the spin waves represent the Goldstone bosons which result from the spontaneously broken internal spin rotation symmetry of the Heisenberg [$O(3) \rightarrow O(2)$] and the XY model [$O(2) \rightarrow 1$], respectively. It is important to note that, at finite temperature, spontaneous symmetry breaking in two (or less) spatial dimensions cannot occur due to the Mermin-Wagner theorem [10]. Nonetheless, the spin waves still dominate the physics of the system at low temperatures.

Many articles have addressed the behavior of the quantum XY model in two spatial dimensions near or at the Kosterlitz-Thouless phase transition, which takes place around $T_{KT} \approx 0.343J$ for the square lattice [11], J being the exchange coupling. On the other hand, the thermodynamic properties in the regime $T < T_{KT}$, where the spin-waves are the relevant excitations, have only been explored scarcely [12–17]. In particular, the effect of the spin-wave interaction on the low-temperature properties of the quantum XY model in two spatial dimensions has not been considered so far, to the best of our knowledge.

In Refs. [18–20] the thermodynamic behavior of systems with a spontaneously broken global symmetry $O(N) \rightarrow O(N-1)$ has been analyzed up to two loops in the effective expansion. In the present study we go one step farther in the low-temperature expansion by including three-loop effects. The calculation for the general case $O(N) \rightarrow O(N-1)$, and for two spatial dimensions, has been presented in Ref. [21]. That article, however, focused on the special case $N=3$, i.e., on the antiferromagnetic Heisenberg model and did not discuss the physics of the quantum XY model which is the main topic of the present work.

We emphasize that the results for the quantum XY model presented below do not just correspond to adapting the formulas derived earlier for general N in Ref. [21] to the case $N=2$. Rather, we have to renormalize and numerically evaluate a particular contribution in a three-loop graph which was not relevant for the $d=2+1$ antiferromagnet. In the $d=2+1$ quantum XY model this term in fact represents one of the essential contributions coming from the spin-wave interaction.

The main goal of our systematic three-loop calculation is to answer the question of how the spin-wave interaction manifests itself in various thermodynamic quantities at low temperatures, and how these results are influenced by an external magnetic or staggered field. As it turns out, the spin-wave interaction is repulsive at low temperatures, its magnitude depending on the strength of the external field. It will be very instructive to compare these findings with those referring to the $d=2+1$ Heisenberg antiferromagnet. We emphasize that our systematic three-loop calculation appears to be beyond the reach of conventional methods such as spin-wave theory – or would require such an immense effort that it would not be worthwhile trying to solve the problem with microscopic methods.

We then discuss in which parameter regime the series derived in this work are valid. On the one hand, our effective results are restricted to temperatures low compared to the underlying microscopic scale, given by the exchange integral J . In the case of the antiferromagnetic Heisenberg model the domain of validity is also restricted due to the nonperturbatively generated mass gap.

Recently, both the quantum XY model and the antiferromagnetic Heisenberg model in two spatial dimensions have been analyzed numerically in Refs. [22, 23], where high-precision measurements using the very effective loop-cluster algorithm were presented. Comparing these numerical results with analytic two-loop calculations obtained within effective field theory, permitted to extract some combinations of low-energy constants at the permille level – above all, it demonstrated the correctness of the effective field theory approach for these systems whose low-energy physics is dominated by spin waves.

In order to promote the effective Lagrangian method, we would like to provide the interested reader with a series of articles where this method has been used to address condensed matter problems. These systematic studies include antiferromagnets and ferromagnets in three [24–31], two [18–21, 32, 33] and one [34, 35] spatial dimensions, as well as two-dimensional antiferromagnets which turn into high-temperature superconductors upon doping [36–43].

The rest of the paper is organized as follows. In Sec. 2 we provide a brief outline of the effective Lagrangian description of the quantum XY model. The evaluation of the partition function up to three-loop order in the low-temperature expansion is presented in Sec. 3. The low-temperature series for various thermodynamic quantities, including the order parameter, are derived in Sec. 4 for the $(2+1)$ -d quantum XY model. In particular, the impact of the external field on the spin-wave interaction is discussed there. In Sec. 5 we compare these results with those describing the $(2+1)$ -d Heisenberg antiferromagnet. Finally, our conclusions are presented in Sec. 6, and some technical details regarding the effective description of Heisenberg and XY magnets, as well as the renormalization and numerical evaluation of a particular three-loop graph are discussed in Appendices A and B.

2 Effective Field Theory for the D=2+1 Quantum XY Model

On the microscopic level, the quantum XY model in two spatial dimensions is described by the Hamiltonian

$$\mathcal{H} = -J \sum_{\langle xy \rangle} (S_x^1 S_y^1 + S_x^2 S_y^2) - \vec{H} \cdot \sum_x \vec{S}_x, \quad J > 0. \quad (2.1)$$

We assume that the lattice is bipartite, where x and y represent nearest-neighbor lattice sites with spacing a . J is the ferromagnetic exchange coupling constant. The spin- $\frac{1}{2}$ operators \vec{S}_x follow the standard commutation relations

$$[S_x^a, S_y^b] = i\delta_{xy}\varepsilon_{abc}S_x^c. \quad (2.2)$$

Note that, contrary to the Heisenberg model, only the generator S^3 commutes with the Hamiltonian. The quantity $\vec{H} = (0, H)$ represents a weak external magnetic field which is restricted to the XY-plane and couples to the magnetization order parameter \vec{S} ,

$$\vec{S} = \left(\sum_x S_x^1, \sum_x S_x^2 \right). \quad (2.3)$$

At infinite volume and zero temperature, the vacuum expectation value of its second component is different from zero,

$$\Sigma = \langle 0 | \sum_x S_x^2 | 0 \rangle / V, \quad (2.4)$$

indicating that the $O(2)$ spin symmetry is spontaneously broken.

On a bipartite lattice, and in the absence of an external field, the antiferromagnetic quantum XY model is related to the ferromagnetic one by a unitary transformation. In fact, the mapping also holds if we allow for external fields, as we show now. Applying the similarity transformation [6]

$$S_x^1 \rightarrow -S_x^1, \quad S_x^2 \rightarrow -S_x^2, \quad S_x^3 \rightarrow S_x^3, \quad (2.5)$$

on every site x of the odd sublattice, the ferromagnetic XY Hamiltonian turns into

$$\mathcal{H} = J \sum_{\langle xy \rangle} (S_x^1 S_y^1 + S_x^2 S_y^2) - \vec{H} \cdot \sum_x (-1)^x \vec{S}_x, \quad J > 0. \quad (2.6)$$

This Hamiltonian describes the antiferromagnetic XY model in the presence of the field \vec{H} , which we now interpret as staggered field \vec{H}_s in the XY-plane, as it couples to the staggered magnetization order parameter $\sum_x (-1)^x \vec{S}_x$. There is thus a one-to-one correspondence between the XY ferromagnet in a magnetic field and the XY antiferromagnet in a staggered field on a bipartite lattice. From now on, in order to compare

our results with the Heisenberg antiferromagnet, we stick to "antiferromagnetic XY language".

The systematic effective Lagrangian method is designed for systems which display a spontaneously broken global symmetry. In the case of the quantum XY model, the continuous spin symmetry $O(2)$ is spontaneously broken by the ground state to 1 at $T = 0$. The antiferromagnetic Heisenberg model, on the other hand, follows the pattern $O(3) \rightarrow O(2)$. As a consequence of Goldstone's theorem, the low-energy dynamics of both systems is governed by the spin-waves or magnons, which are characterized by a linear, i.e., relativistic dispersion relation.

Essential aspects of the effective Lagrangian technique and the perturbative evaluation of the partition function have been outlined on various occasions, such that here we only provide a minimum of information needed to understand the present calculation. More details can be found in Section 2 of Ref. [21] and in appendix A of Ref. [31]. Furthermore, pedagogic introductions to the effective field theory are provided in Refs. [44–49].

In the quantum XY model, the relevant excitation at low energies is the magnon. It is convenient to define a unit vector field $U^i(x)$,

$$U^i(x)U^i(x) = 1, \quad i = 1, 2, \quad (2.7)$$

which contains the Goldstone boson field in its first component U^1 . Remember that we have chosen the weak external field to point along the 2-direction, $\vec{H}_s = (0, H_s)$. Accordingly the spin waves represent fluctuations orthogonal to this direction.

The organization of the effective Lagrangian is based on the number of time and space derivatives the various terms display. Terms with few derivatives dominate the low-energy physics of the system, while terms containing more derivatives are less important. We are thus dealing with a systematic expansion in powers of energy and momenta. The leading-order effective Lagrangian of the quantum XY model contains terms with two time ($\partial_0\partial_0$) and two space ($\partial_r\partial_r$) derivatives,

$$\mathcal{L}_{eff}^2 = \frac{1}{2}F_1^2\partial_0U^i\partial_0U^i - \frac{1}{2}F_2^2\partial_rU^i\partial_rU^i + \Sigma_s H_s^i U^i \quad (2.8)$$

$$r = 1, 2,$$

as well as a term containing the external staggered field H_s^i and the constant Σ_s which is the staggered magnetization at zero temperature and infinite volume. All these contributions are of momentum order p^2 and lead to a relativistic dispersion relation,

$$\omega = \sqrt{v^2\vec{k}^2 + v^4M^2}, \quad v = \frac{F_2}{F_1}, \quad (2.9)$$

where the quantity v is the spin-wave velocity. If one identifies the spin-wave velocity with the velocity of light, the leading-order effective Lagrangian becomes (pseudo-) Lorentz invariant. Setting $v \equiv 1$, we may use relativistic notation,

$$\mathcal{L}_{eff}^2 = \frac{1}{2}F^2\partial_\mu U^i\partial^\mu U^i + \Sigma_s H_s^i U^i, \quad F_1 = F_2 = F. \quad (2.10)$$

The quantity M in the dispersion relation is then interpreted as the "mass" of the magnon, i.e., the energy gap in the spectrum, which is related to the external field by

$$M^2 = \frac{\Sigma_s H_s}{F^2}. \quad (2.11)$$

Note that (pseudo-)Lorentz invariance is an accidental symmetry of \mathcal{L}_{eff}^2 , which is not shared by the microscopic XY model. Moreover, the symmetry only emerges at leading order in the derivative expansion – higher-order contributions in the effective Lagrangian explicitly break (pseudo-)Lorentz invariance. In fact, they also break O(2) space rotation symmetry due to the anisotropies of the underlying lattice which start manifesting themselves at order p^4 . In the present paper, however, we assume (pseudo-)Lorentz invariance also at next-to-leading order \mathcal{L}_{eff}^4 , and thus obtain [18]:

$$\begin{aligned} \mathcal{L}_{eff}^4 &= e_1(\partial_\mu U^i \partial^\mu U^i)^2 + e_2(\partial_\mu U^i \partial^\nu U^i)^2 \\ &+ k_1 \frac{\Sigma_s}{F^2} (H_s^i U^i) (\partial_\mu U^k \partial^\mu U^k) + k_2 \frac{\Sigma_s^2}{F^4} (H_s^i U^i)^2 \\ &+ k_3 \frac{\Sigma_s^2}{F^4} H_s^i H_s^i. \end{aligned} \quad (2.12)$$

It is important to point out that the conclusions of the present paper are not affected by this idealization, as we explore in the following sections.

At leading order (p^2) we have two coupling constants, F and Σ_s , while at next-to-leading order (p^4) five constants, e_1, e_2, k_1, k_2 and k_3 , are required to describe the (anti)ferromagnetic quantum XY model within effective field theory. In contrast to the derivative structure of the terms in the effective Lagrangian, symmetry does not fix these coupling constants which parametrize the physics of the underlying microscopic quantum XY model. Rather, they have to be determined experimentally or in a numerical simulation. Using magnetic terminology, the square of the effective coupling constant F is the spin stiffness or helicity modulus. While the quantities Σ_s and H_s^i represent the staggered magnetization and the staggered external field in the case of the antiferromagnetic XY model, we may also interpret them as magnetization and external magnetic field of the ferromagnetic XY model, provided that the underlying microscopic lattice is bipartite.

In Appendix A we show that on the effective level as well, there is a one-to-one mapping between the ferromagnetic quantum XY model in a magnetic field and the antiferromagnetic quantum XY model in a staggered field for bipartite lattices. Note that there is no such mapping between the ferromagnetic and antiferromagnetic Heisenberg model. Indeed, as is well-known, the Heisenberg ferromagnet is different, the magnons displaying a quadratic dispersion relation. This essential difference between the quantum XY and the Heisenberg model, as outlined in Appendix A, can be traced back to the nature of the spontaneously broken symmetry: while the group O(2) is Abelian, the group O(3) is non-Abelian.

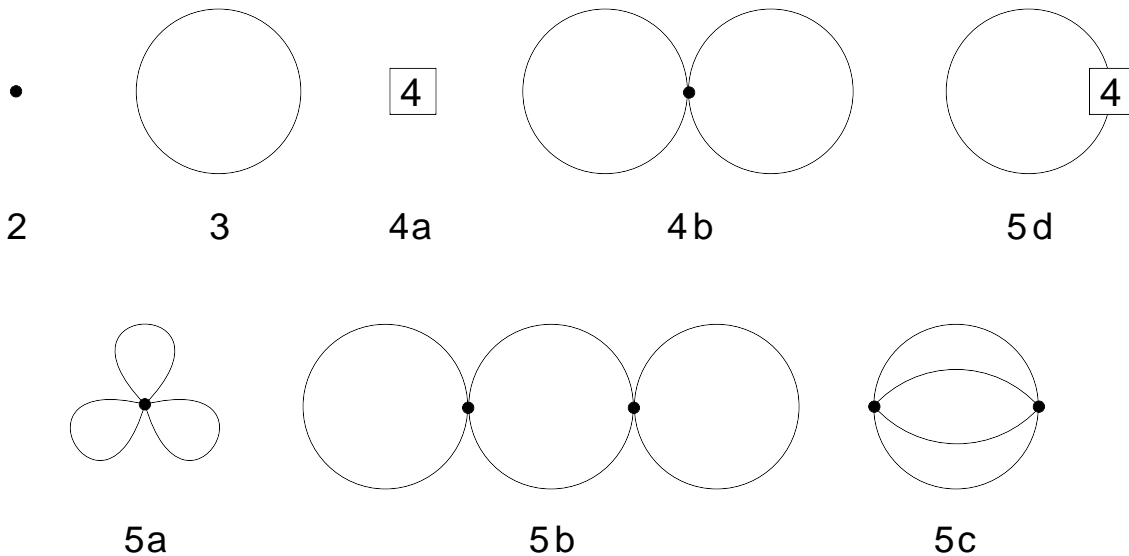


Figure 1: Feynman diagrams referring to the low-temperature expansion of the partition function of $d=2+1$ (pseudo-)Lorentz-invariant systems with a spontaneously broken symmetry $O(N) \rightarrow O(N-1)$ up to three-loop order. Vertices associated with the leading term in the effective Lagrangian, \mathcal{L}_{eff}^2 , are denoted by a filled circle, while vertices involving \mathcal{L}_{eff}^4 are referred to by the number four.

3 Free Energy Density up to Three-Loop Order

The partition function for $(2+1)$ -dimensional (pseudo-)Lorentz-invariant systems with a spontaneously broken global symmetry $O(N) \rightarrow O(N-1)$ [at $T = 0$] has been evaluated within the effective Lagrangian framework up to three-loop order in Ref. [21]. For the Heisenberg antiferromagnet ($N=3$), the rather nontrivial part performed in that reference was the renormalization and numerical evaluation of a specific three-loop graph. In the present case of the quantum XY model ($N=2$) a different three-loop contribution, as will become clear below, emerges which needs to be renormalized and evaluated numerically. This quite elaborate calculation, not needed for the antiferromagnet, is presented in detail in Appendix B, as it is rather technical.

We briefly review the essential results derived in Ref. [21], required for the subsequent discussion. However, in order not to be repetitive, we do not review the evaluation of Feynman graphs at finite temperature. The interested reader may consult Ref. [21] or appendix A of Ref. [31] and the various references given therein.

Up to three-loop order, the eight Feynman diagrams depicted in Fig. 1 are relevant. The sum of these contributions leads to the following expression for the free energy

density for general $N \geq 2$,

$$\begin{aligned}
z &= z_0 - \frac{N-1}{2} h_0(\sigma) T^3 + \frac{(N-1)(N-3)}{8F^2\tau^2} h_1(\sigma)^2 T^4 \\
&- \frac{(N-1)(N-3)(5N-11)}{128\pi F^4\tau^3} h_1(\sigma)^2 T^5 + \frac{(N-1)(N-3)(3N-7)}{48F^4\tau^2} h_1(\sigma)^3 T^5 \\
&- \frac{(N-1)(N-3)^2}{16F^4\tau^4} h_1(\sigma)^2 h_2(\sigma) T^5 + \frac{1}{F^4} q(\sigma) T^5 + \mathcal{O}(T^6),
\end{aligned} \tag{3.1}$$

where z_0 represents the free energy density at zero temperature. The dimensionless quantities σ and τ ,

$$\sigma = \frac{M_\pi}{2\pi T}, \quad \tau = \frac{T}{M_\pi}, \tag{3.2}$$

involve the renormalized mass M_π of the pseudo-Goldstone bosons,

$$\begin{aligned}
M_\pi^2 &= M^2 - \frac{N-3}{8\pi} \frac{M^3}{F^2} \\
&+ \left\{ 2(k_2 - k_1) + \frac{b_1}{F^2} + \frac{b_2}{64\pi^2 F^2} \right\} \frac{M^4}{F^2} + \mathcal{O}(M^5),
\end{aligned} \tag{3.3}$$

which contains higher-order corrections to the leading term

$$M^2 = \frac{\Sigma_s H_s}{F^2}. \tag{3.4}$$

The renormalized mass M_π thus depends on the external field H_s ,

$$\begin{aligned}
M_\pi^2(H_s) &= \frac{\Sigma_s H_s}{F^2} - \frac{N-3}{8\pi} \frac{\Sigma_s^{3/2} H_s^{3/2}}{F^5} \\
&+ \left\{ 2(k_2 - k_1) + \frac{b_1}{F^2} + \frac{b_2}{64\pi^2 F^2} \right\} \frac{\Sigma_s^2 H_s^2}{F^6} \\
&+ \mathcal{O}(H_s^{5/2}).
\end{aligned} \tag{3.5}$$

The coefficients b_1 and b_2 are given by

$$\begin{aligned}
b_1 &= \frac{1}{24}(N-3)\gamma_2 - \frac{1}{2}(N-2)\gamma_4, \\
b_2 &= (N-3)(2N-5).
\end{aligned} \tag{3.6}$$

The quantities γ_2 and γ_4 are singular functions of the space-time dimension d – the explicit expressions can be found in Ref. [21]. The essential point is that the infinities in b_1 , which originate from the three-loop graph 5c, are removed by the combination $k_2 - k_1$ of next-to-leading-order coupling constants, stemming from the one-loop graph 5d. As a consequence, the curly bracket in Eq. (3.5) is free of singularities.

The dimensionless kinematical functions h_0, h_1 and h_2 , defined by

$$g_0 = T^3 h_0(\sigma), \quad g_1 = T h_1(\sigma), \quad g_2 = \frac{1}{T} h_2(\sigma), \tag{3.7}$$

are related to the functions $g_r(M, T)$ which represent Bose functions in d space-time dimensions,

$$g_r(M, T) = 2 \int_0^\infty \frac{d\rho}{(4\pi\rho)^{d/2}} \rho^{r-1} \exp(-\rho M^2) \times \sum_{n=1}^\infty \exp(-n^2/4\rho T^2). \quad (3.8)$$

The dimensionless quantity q ,

$$T^5 q(\sigma) \equiv \frac{1}{48}(N-1)(N-3)M_\pi^4 \bar{J}_1 - \frac{1}{4}(N-1)(N-2)\bar{J}_2, \quad (3.9)$$

involves the renormalized integrals \bar{J}_1 and \bar{J}_2 ,

$$\begin{aligned} \bar{J}_1 &= J_1 - c_1 - c_2 g_1(M, T), \\ \bar{J}_2 &= J_2 - c_3 - c_4 g_1(M, T), \end{aligned} \quad (3.10)$$

which originate from the three-loop graph 5c. The unrenormalized and thus singular integrals J_1 and J_2 are given by

$$\begin{aligned} J_1 &= \int_{\mathcal{T}} d^d x \{G(x)\}^4, \\ J_2 &= \int_{\mathcal{T}} d^d x \{\partial_\mu G(x) \partial_\mu G(x)\}^2. \end{aligned} \quad (3.11)$$

Here, $G(x)$ is the thermal propagator,

$$G(x) = \sum_{n=-\infty}^\infty \Delta(\vec{x}, x_4 + n\beta), \quad (3.12)$$

and $\Delta(x)$ represents the zero-temperature Euclidean propagator,

$$\begin{aligned} \Delta(x) &= (2\pi)^{-d} \int d^d p e^{ipx} (M^2 + p^2)^{-1} \\ &= \int_0^\infty d\rho (4\pi\rho)^{-d/2} e^{-\rho M^2 - x^2/4\rho}, \end{aligned} \quad (3.13)$$

dimensionally regularized in the space-time dimension d . The coefficients c_1, \dots, c_4 in Eq. (3.10) are subtraction constants which absorb the infinities in the integrals J_1 and J_2 – the explicit representations can be found in appendix A of Ref. [21] and in appendix B of the present article. Inspecting Eq. (3.9), it becomes evident that while the contribution \bar{J}_2 is relevant for the Heisenberg model, for the quantum XY model it is the contribution \bar{J}_1 that matters – this is the new expression we have to renormalize and evaluate numerically (see appendix B).

For general $N \geq 2$, according to Eq. (3.1), the leading contribution in the free energy density is of order T^3 and represents the free Bose gas term, corresponding to the

one-loop graph 3. The dominant interaction term is of order T^4 and originates from the two-loop graph 4b. At order T^5 we have a total of three three-loop graphs that contribute to the interaction, all of them involving the leading-order Lagrangian \mathcal{L}_{eff}^2 only. Note that we are dealing with a series characterized by integer powers of the temperature, the leading contribution of order T^3 receiving corrections of ascending powers of T . This is a consequence of the fact that (i) each additional loop in a Feynman diagram corresponds to one additional power of $p \propto T$ in two spatial dimensions and that (ii) the spin waves are characterized by a linear dispersion relation.

For the d=2+1 quantum XY model ($N=2$), the free energy density (3.1) reads

$$\begin{aligned} z^{\text{XY}} &= z_0^{\text{XY}} - \frac{1}{2}h_0(\sigma)T^3 - \frac{1}{8F^2\tau^2}h_1^2(\sigma)T^4 \\ &- \frac{1}{128\pi F^4\tau^3}h_1^2(\sigma)T^5 + \frac{1}{48F^4\tau^2}h_1^3(\sigma)T^5 \\ &- \frac{1}{16F^4\tau^4}h_1^2(\sigma)h_2(\sigma)T^5 + \frac{1}{F^4}q^{\text{XY}}(\sigma)T^5 + \mathcal{O}(T^6). \end{aligned} \quad (3.14)$$

The leading contribution due to the spin-wave interaction is of order T^4 , subsequent corrections are of order T^5 .

Interestingly, for the d=2+1 Heisenberg antiferromagnet ($N=3$), many terms in Eq. (3.1) vanish and the free energy density takes the simple form

$$z^{\text{AF}} = z_0^{\text{AF}} - h_0(\sigma)T^3 + \frac{1}{F^4}q^{\text{AF}}(\sigma)T^5 + \mathcal{O}(T^6). \quad (3.15)$$

Here, unlike for the spin waves in the quantum XY model, the interaction starts manifesting itself only at order T^5 .

For the above low-temperature series to be valid, it is important that the quantities T and M_π (i.e., the external field H_s) are small compared to the intrinsic scale defined by the underlying microscopic theory. This scale is given by the exchange integrals J of the quantum XY and the Heisenberg model. While the ratios $\sigma = M_\pi/2\pi T$ and $\tau = T/M_\pi$ can take any values in three spatial dimensions, restrictions are imposed in two spatial dimensions. In particular, as we discuss in the next section, the external field H_s cannot be switched off completely.

We emphasize that anisotropies due to the geometry of the underlying microscopic lattice only show up at higher orders of the derivative expansion in the effective theory. The different discrete symmetries of e.g. the square and the honeycomb lattice, only manifest themselves at order p^4 in the effective Lagrangian. These space-anisotropies do not affect the main conclusions of the present paper – and a (pseudo-)Lorentz-invariant framework, even at next-to-leading order of the derivative expansion, is perfectly justified as we further underline in the next section.

4 Low-Temperature Series for the D=2+1 Quantum XY Model

We now provide the low-temperature expansions for various thermodynamic quantities, including the order parameter. In particular, we explore how the strength of the spin-wave interaction depends on the magnitude of the external field and on temperature, and answer the question in which regions of parameter space, defined by T , M_π (i.e., H_s) and F , our effective expansions are valid.

Up to three loops, the pressure for the d=2+1 quantum XY model takes the form

$$\begin{aligned}
 P^{\text{XY}} &= z_0^{\text{XY}} - z^{\text{XY}} = \frac{1}{2}h_0(\sigma)T^3 + \frac{1}{8F^2\tau^2}h_1(\sigma)^2T^4 \\
 &+ \frac{1}{128\pi F^4\tau^3}h_1(\sigma)^2T^5 - \frac{1}{48F^4\tau^2}h_1(\sigma)^3T^5 \\
 &+ \frac{1}{16F^4\tau^4}h_1(\sigma)^2h_2(\sigma)T^5 - \frac{1}{F^4}q^{\text{XY}}(\sigma)T^5 + \mathcal{O}(T^6).
 \end{aligned} \tag{4.1}$$

The function $q(\sigma)$, defined in Eq. (3.9), is depicted for $N=2$ in Fig. 2. It develops a minimum around $\sigma \approx 0.22$ and tends to zero both for small and large values of σ . Expressions suitable for the numerical evaluation of $q(\sigma)$ are given in Appendix B. Roughly speaking, according to Eq. (3.5), the parameter $\sigma = M_\pi/2\pi T$ is proportional to $\sqrt{H_s}/T$, i.e., the ratio between the square root of the external field and the temperature.

The leading interaction contribution of order T^4 in the pressure is positive, signaling that the interaction between spin waves is repulsive. The sum of the three-loop corrections of order T^5 slightly enhances the repulsive interaction, as can be appreciated in Fig. 3. The interaction is strongest at the value $\sigma \approx 0.11$. According to Fig. 4, this maximum is basically independent of the ratio T/F^2 .

Now on the square lattice we have $F^2 = 0.26974(5)J$ [23], which is close to the Kosterlitz-Thouless transition temperature $T_{KT} \approx 0.343J$. Both quantities, F^2 and T_{KT} , are of the order of the underlying microscopic scale J . For our effective expansions to be valid, the ratio T/F^2 must thus be small. The value $\sigma \approx 0.11$, using the first two terms on the RHS of Eq. (3.5), corresponds to $H_s/T^2 \approx 0.38/J$ for the square lattice. For this ratio of external field versus temperature squared, the magnitude of the spin-wave interaction in the pressure is largest. Again, these results apply to the quantum XY model on the square lattice, where the other low-energy constants take the values $\Sigma_s = 0.43561(1)/a^2$ and $v = 1.1347(2)Ja$ [23].

An important comment on (pseudo-)Lorentz invariance and lattice anisotropies is in order here. As we have pointed out, the leading-order effective Lagrangian \mathcal{L}_{eff}^2 Eq. (2.8) displays an accidental O(2) space rotation symmetry and can thus be written in a (pseudo-)Lorentz-invariant form. We then have assumed that this

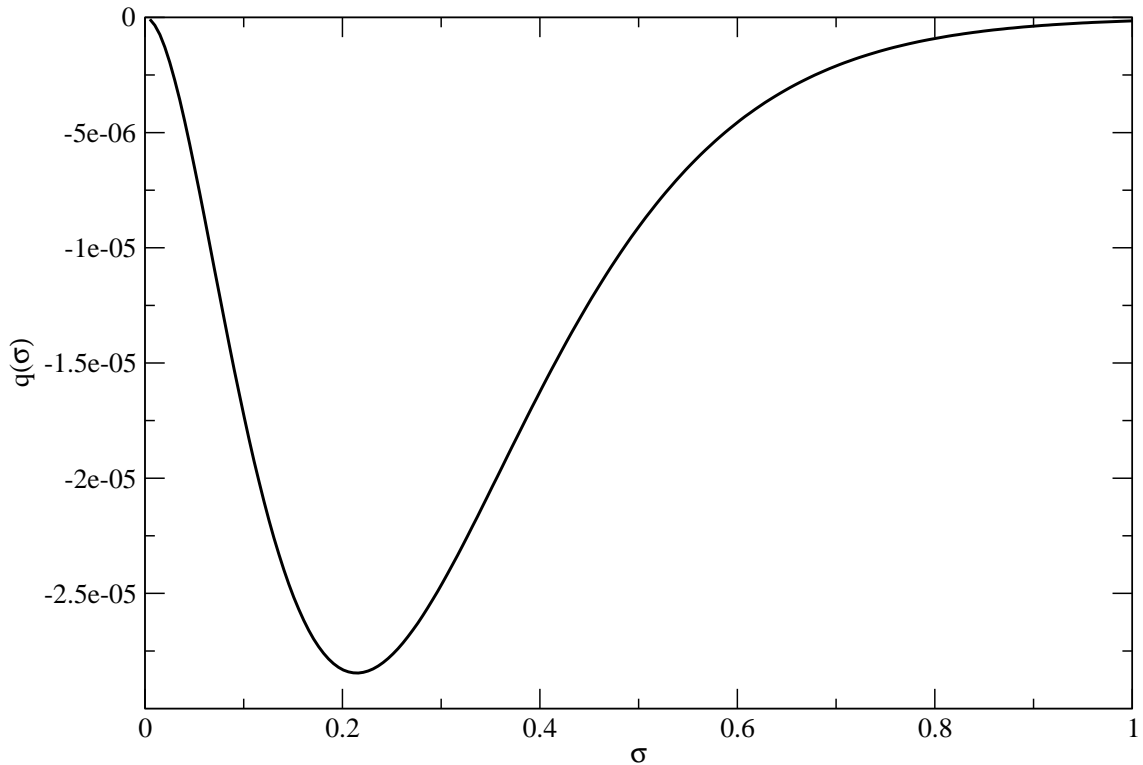


Figure 2: The function $q(\sigma)$ for $N=2$, with $\sigma = M_\pi/2\pi T$ as dimensionless parameter.

symmetry persists at order \mathcal{L}_{eff}^4 . This idealization is indeed well-justified, as the only place where these Lorentz-symmetry breaking effects manifest themselves in the temperature-dependent quantities, is through the one-loop diagram 5d of Fig. 1. This specific diagram only affects the renormalized mass and does so only at next-to-next-to-leading order in the form of the subleading low-energy constants k_1 and k_2 in Eq. (3.5). From this point of view, the differences between e.g. the square and the honeycomb lattice are negligible, as they correspond to a next-to-next-to-leading order effect which does not affect at all our conclusions.

A crucial point, on the other hand, is to realize that the geometry of the lattice does manifest itself in a rather trivial way. Although the leading-order effective Lagrangian \mathcal{L}_{eff}^2 is (pseudo-)Lorentz invariant – again, this is a rigorous statement – the actual values of the low-energy constants Σ_s (staggered magnetization at zero temperature and zero external field), v (spin-wave velocity) and F^2 (spin stiffness or helicity modulus) depend on the lattice geometry. While the structure of the low-temperature series, i.e. the specific powers of the temperature involved and the dependence on the external field, is universal for bipartite lattices, the differences between various lattice geometries show up in the coefficients of these series, as they depend on the low-energy constants.

To further explore the effect of the spin-wave interaction, we also consider the

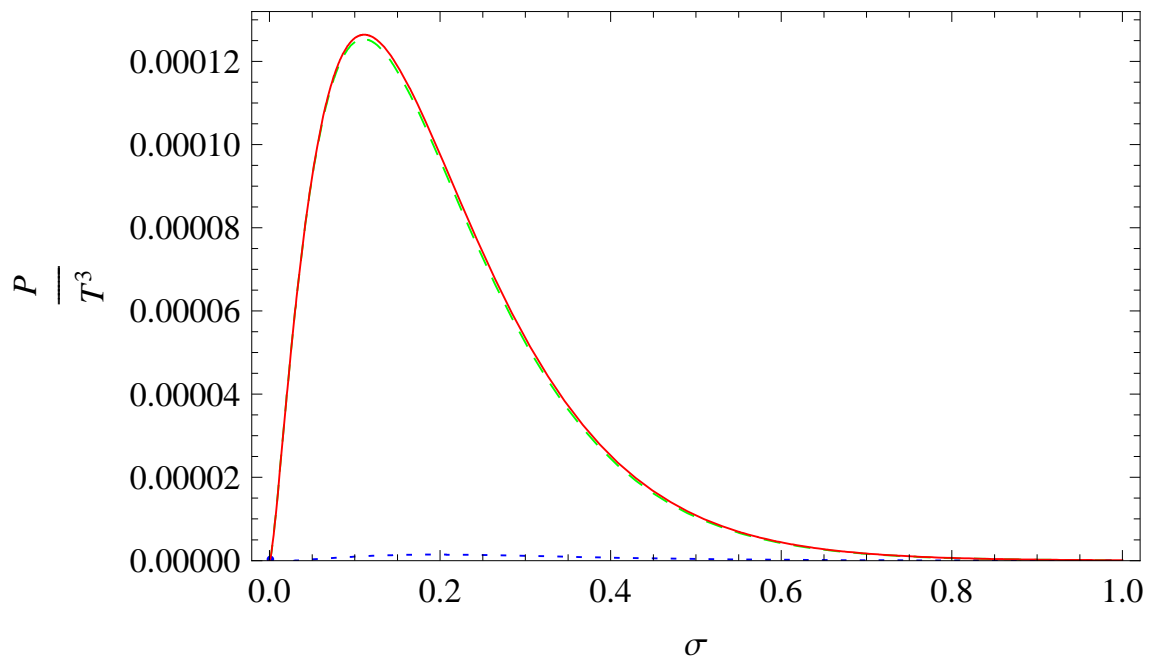


Figure 3: (2+1)-dimensional quantum XY model: Interaction corrections to the pressure as a function of the dimensionless ratio $\sigma = M_\pi/2\pi T$, evaluated at $T/F^2 = \frac{1}{2}T_{KT}/J$, where $T_{KT} \approx 0.343J$ is the Kosterlitz-Thouless transition temperature. The two-loop contribution (dashed curve) is slightly enhanced by the three-loop contribution (dotted curve). The sum (continuous curve) develops a maximum around $\sigma = 0.11$.

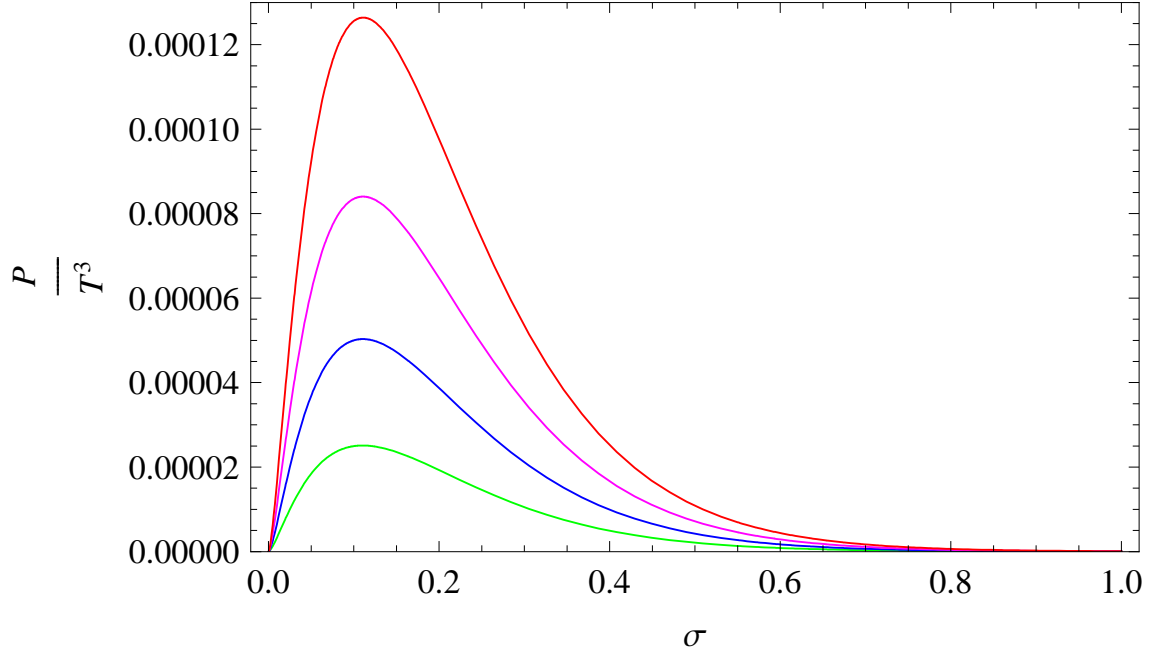


Figure 4: (2+1)-dimensional quantum XY model: The sum of the two-loop and three-loop corrections to the pressure as a function of $\sigma = M_\pi/2\pi T$, evaluated at $T/F^2 = \{\frac{1}{10}, \frac{1}{5}, \frac{1}{3}, \frac{1}{2}\}T_{KT}/J$, from bottom to top in the figure.

order parameter. The low-temperature expansion of the staggered magnetization,

$$\Sigma_s(T, H_s) = -\frac{\partial z}{\partial H_s}, \quad (4.2)$$

amounts to

$$\begin{aligned} \Sigma_s^{\text{XY}}(T, H_s) &= \Sigma_s^{\text{XY}}(0, H_s) - \frac{\Sigma_s b}{2F^2} h_1(\sigma) T + \frac{\Sigma_s b}{8F^4} \left\{ h_1(\sigma)^2 - \frac{2}{\tau^2} h_1(\sigma) h_2(\sigma) \right\} T^2 \\ &+ \frac{\Sigma_s b}{128\pi F^6} \left\{ \frac{3}{2\tau} h_1(\sigma)^2 - \frac{2}{\tau^3} h_1(\sigma) h_2(\sigma) \right\} T^3 - \frac{\Sigma_s b}{48F^6} \left\{ h_1(\sigma)^3 - \frac{3}{\tau^2} h_1(\sigma)^2 h_2(\sigma) \right\} T^3 \\ &+ \frac{\Sigma_s b}{16F^6} \left\{ \frac{2}{\tau^2} h_1(\sigma)^2 h_2(\sigma) - \frac{2}{\tau^4} h_1(\sigma) h_2(\sigma)^2 - \frac{1}{\tau^4} h_1(\sigma)^2 h_3(\sigma) \right\} T^3 \\ &- \frac{\Sigma_s b}{8\pi^2 F^6 \sigma} \frac{\partial q^{\text{XY}}(\sigma)}{\partial \sigma} T^3 + \mathcal{O}(T^4). \end{aligned} \quad (4.3)$$

The quantity b , for general N , is defined by

$$\begin{aligned} b(H_s) &= \frac{\partial M_\pi^2}{\partial M^2} = 1 - \frac{3(N-3)\sqrt{\Sigma_s}}{16\pi F^3} \sqrt{H_s} + \frac{2\tilde{k}_0 \Sigma_s}{F^4} H_s \\ &+ \mathcal{O}(H_s^{3/2}), \\ \tilde{k}_0 &= 2(k_2 - k_1) + \frac{b_1}{F^2} + \frac{b_2}{64\pi^2 F^2}. \end{aligned} \quad (4.4)$$

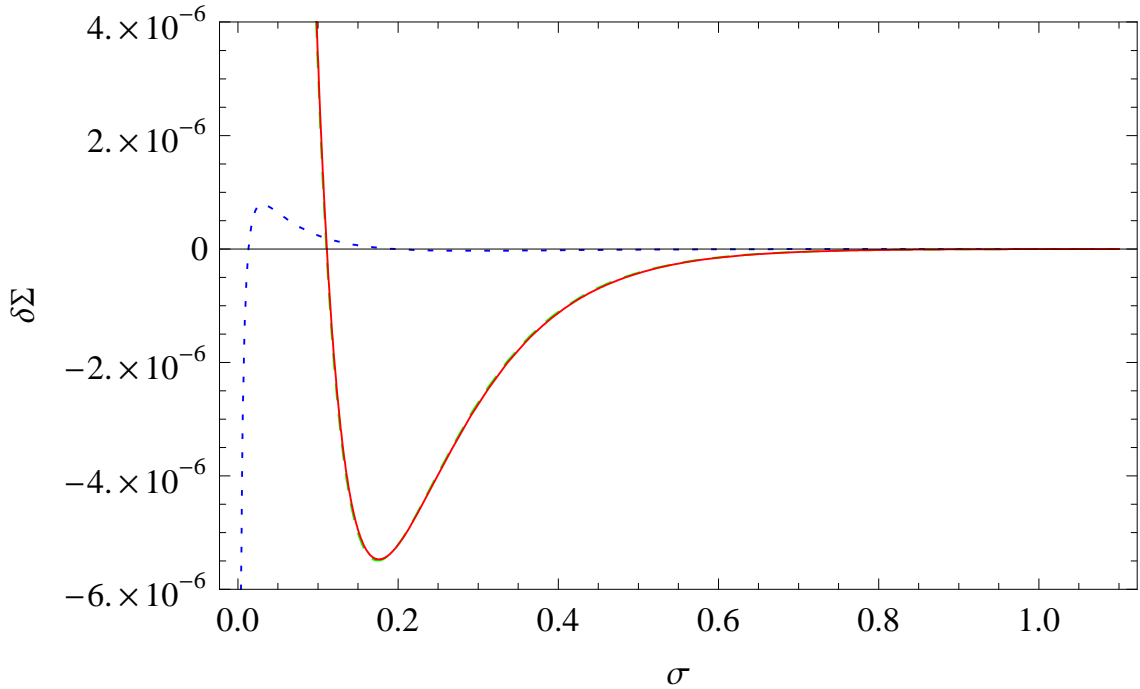


Figure 5: (2+1)-dimensional quantum XY model: Temperature-dependent interaction corrections to the staggered magnetization, $\delta\Sigma_s$, as a function of the dimensionless ratio $\sigma = M_\pi/2\pi T$, evaluated at $T/F^2 = \frac{1}{2}T_{KT}/J$. The two-loop contribution (dashed curve) and three-loop contribution (dotted curve) add up to the total correction (continuous curve) which is negative in the whole parameter region, except for small values of σ .

Inverting Eq. (3.5), i.e., expressing the staggered field H_s as a function of the renormalized mass M_π , the factor b can be rewritten as $b = b(M_\pi)$. This M_π -dependent representation of b will be used in the subsequent plots. Finally, the quantity $\Sigma_s^{\text{XY}}(0, H_s)$ in Eq. (4.3), is the zero-temperature order parameter in the presence of the external field. For general N we have

$$\begin{aligned}\Sigma_s(0, H_s) &= \Sigma_s + \frac{(N-1)\Sigma_s^{3/2}}{8\pi F^3} \sqrt{H_s} + \mathcal{O}(H_s), \\ \Sigma_s &= \Sigma_s^{\text{XY}}(0, 0).\end{aligned}\tag{4.5}$$

Again, inverting Eq. (3.5), $\Sigma_s(0, H_s)$ can be written as a function of M_π . Of course, in the following plots related to the quantum XY model, we have set $N=2$.

Our focus is the impact of the spin-wave interaction in the temperature-dependent part of the staggered magnetization, given by the difference $\Sigma_s^{\text{XY}}(T, H_s) - \Sigma_s^{\text{XY}}(0, H_s)$. A plot of the dimensionless quantity

$$\delta\Sigma_s \equiv \frac{\Sigma_s^{\text{XY}}(T, H_s) - \Sigma_s^{\text{XY}}(0, H_s)}{\Sigma_s},\tag{4.6}$$

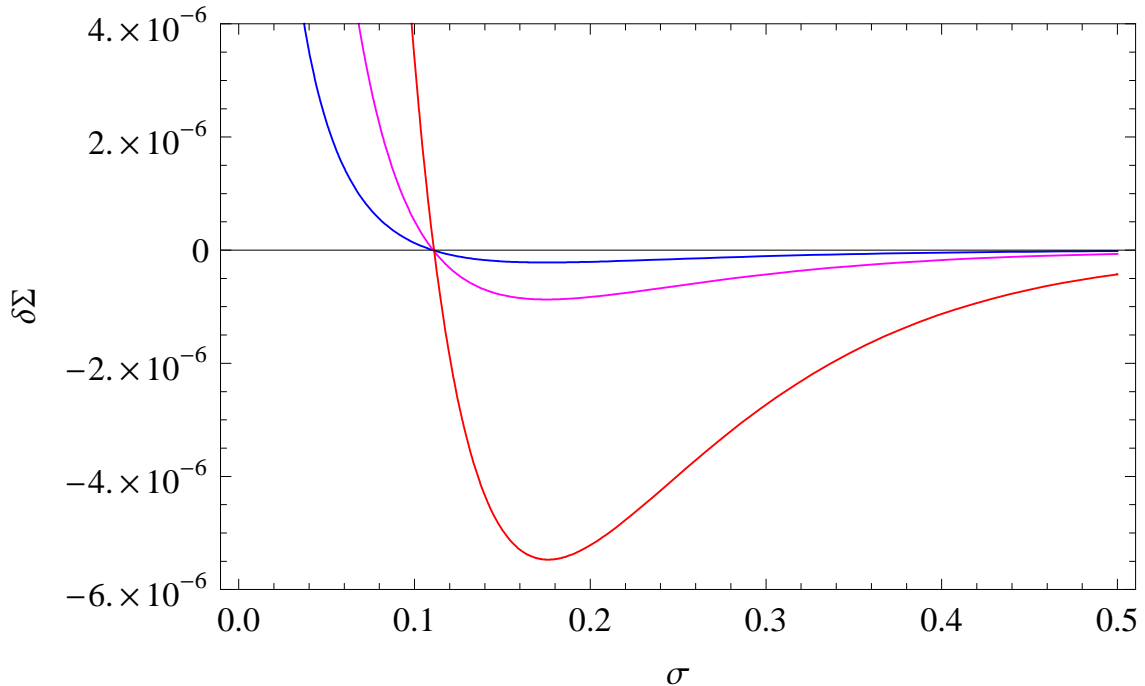


Figure 6: (2+1)-dimensional quantum XY model: The sum of the two-loop and three-loop corrections to the staggered magnetization as a function of the dimensionless ratio $\sigma = M_\pi/2\pi T$, evaluated at $T/F^2 = \{\frac{1}{10}, \frac{1}{5}, \frac{1}{2}\}T_{KT}/J$, from top to bottom in the figure. The quantity $T_{KT} \approx 0.343J$ is the Kosterlitz-Thouless phase transition temperature.

both for the two-loop ($\propto T^2$) and three-loop ($\propto T^3$) contribution in the order parameter Eq. (4.3), is provided in Fig. 5. The sum of these contributions is negative in most of the parameter space, except for small values of σ where the quantity $\delta\Sigma_s$ is positive. Note that the point where the temperature-dependent spin-wave interaction correction vanishes, is basically independent of the ratio T/F^2 , as illustrated in Fig. 6.

In the low-temperature series derived in the present study, the values of the ratios $T/F^2 \propto T/J$ and $H_s/F^2 \propto H_s/J$ must be small – otherwise, we would leave the low-energy domain where the effective expansion applies. However, so far we have not considered the restrictions imposed by the Mermin-Wagner theorem [10]. At finite temperature, in the absence of external fields, there is no spontaneous symmetry breaking in two spatial dimensions. Taking the limit $M_\pi \rightarrow 0$ or, equivalently, switching off the external field in the above low-temperature expansions, is thus problematic.

If we formally take the limit $\sigma \rightarrow 0$ in the pressure, internal energy density, entropy density and heat capacity, all interaction contributions vanish and we are left with

the free magnon part given by

$$\begin{aligned}
P^{\text{XY}} &= \frac{\zeta(3)}{2\pi} T^3 + \mathcal{O}(T^6), \\
u^{\text{XY}} &= \frac{\zeta(3)}{\pi} T^3 + \mathcal{O}(T^6), \\
s^{\text{XY}} &= \frac{3\zeta(3)}{2\pi} T^2 + \mathcal{O}(T^5), \\
c_V^{\text{XY}} &= \frac{3\zeta(3)}{\pi} T^2 + \mathcal{O}(T^5).
\end{aligned} \tag{4.7}$$

Note that the limit $\sigma = M_\pi/2\pi T \rightarrow 0$ is implemented by switching the external field (i.e., M_π) off, while keeping the temperature finite. Formally, this limit poses no problems in the above quantities. However, analyzing the behavior of the order parameter, indicates that there is a subtlety, as we now underline.

The leading terms in the low-temperature expansion of the pressure Eq. (4.1) and the order parameter Eq. (4.3) are proportional to the kinematical function $h_0(\sigma)$ and $h_1(\sigma)$, respectively. Their Taylor expansion in the parameter σ , i.e., for a weak external staggered field, takes the form

$$\begin{aligned}
h_0(\sigma) &= \frac{\zeta(3)}{\pi} - \frac{1}{4\pi} \frac{\Sigma_s H_s}{F^2 T^2} + \frac{1}{4\pi} \frac{\Sigma_s H_s}{F^2 T^2} \ln \frac{\Sigma_s H_s}{F^2 T^2} + \dots, \\
h_1(\sigma) &= -\frac{1}{4\pi} \ln \frac{\Sigma_s H_s}{F^2 T^2} + \dots
\end{aligned} \tag{4.8}$$

Switching off the external field H_s in the order parameter is thus problematic due to the term $\ln H_s$ in $h_1(\sigma)$ which becomes divergent. This is precisely where the Mermin-Wagner theorem enters through the backdoor – the issue is quite subtle. We start by estimating the temperature where our effective series break down. Consider the first two terms in low-temperature expansion of the order parameter Eq. (4.3), i.e. the zero-temperature staggered magnetization in presence of the external field H_s and the leading (one-loop) temperature-dependent contribution. When the staggered magnetization becomes zero, or even takes negative values, the effective expansion can no longer be trusted. This is because the temperature where the effective analysis operates must be smaller than the temperature where the spin-wave picture breaks down. For a given value of the staggered field, we thus get an estimate for this ”critical” temperature T_c , by solving the equation

$$\Sigma_s^{\text{XY}}(T, H_s) = \Sigma_s + \frac{\Sigma_s^{3/2}}{8\pi F^3} \sqrt{H_s} - \frac{\Sigma_s b}{2F^2} h_1(\sigma) T \equiv 0, \tag{4.9}$$

where

$$h_1(\sigma) = -\frac{\ln(1 - e^{-M_\pi/T})}{2\pi} \approx -\frac{\ln(1 - e^{-\sqrt{\Sigma_s H_s}/FT})}{2\pi}. \tag{4.10}$$

On the square lattice, the ratios $H_s/F^2 = \{10^{-1}, 10^{-10}, 10^{-100}, 10^{-1000}, 10^{-10000}\}$ correspond to $T_c/J = \{1.715, 0.3184, 0.03032, 0.002961, 0.0002949\}$. Weakening the staggered field, the ”critical” temperature gradually becomes smaller, and logarithmically

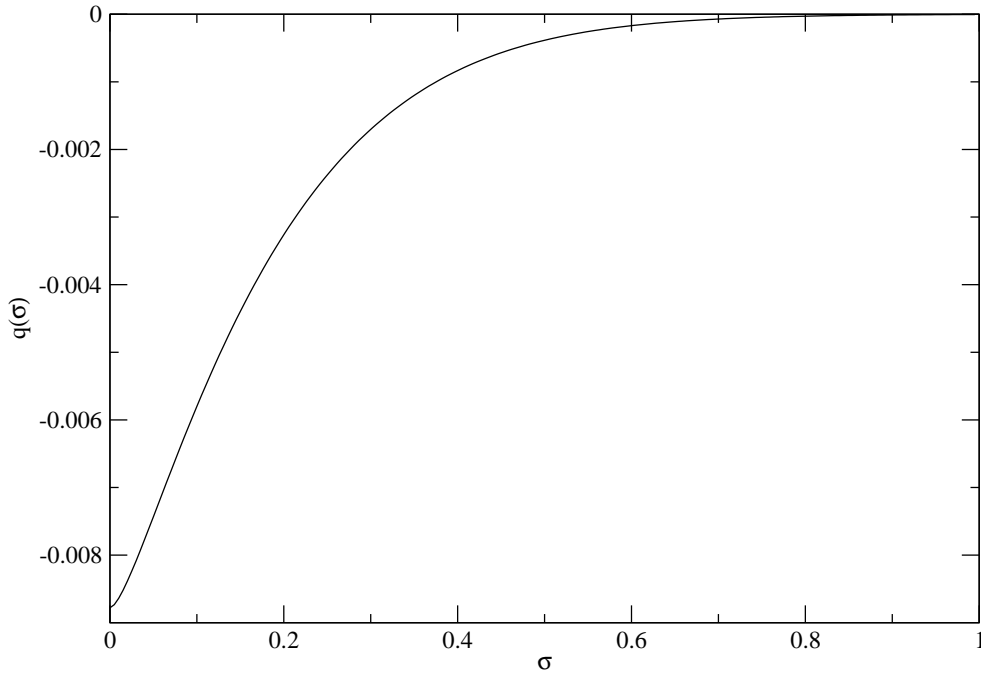


Figure 7: The function $q(\sigma)$ for $N=3$, with $\sigma = M_\pi/2\pi T$ as dimensionless parameter.

tends to zero in the limit $H_s \rightarrow 0$. Hence the temperature range, in which our effective analysis operates, shrinks to zero. The low-temperature representation of the order parameter, Eq. (4.3), then no longer makes sense – the staggered field must always be different from zero.

Note that the problematic term $\ln H_s$ in the order parameter, interestingly, in the thermodynamic quantities P, u, s and c_V manifests itself as $H_s \ln H_s$. Although it is also conceptually inconsistent to take the limit $H_s \rightarrow 0$ in these quantities, there is no divergent behavior. In fact, for a given set of H_s/F^2 and T_c provided above, the ratio $\Sigma_s H_s/F^2 T_c^2$ is tiny, such that the first term in the expansion of h_0 , Eq. (4.8), dominates over the remainder. As a consequence, neglecting the nonleading terms altogether does not really numerically affect the low-temperature series for P, u, s and c_V . Therefore the results displayed in Eq. (4.7) are correct.

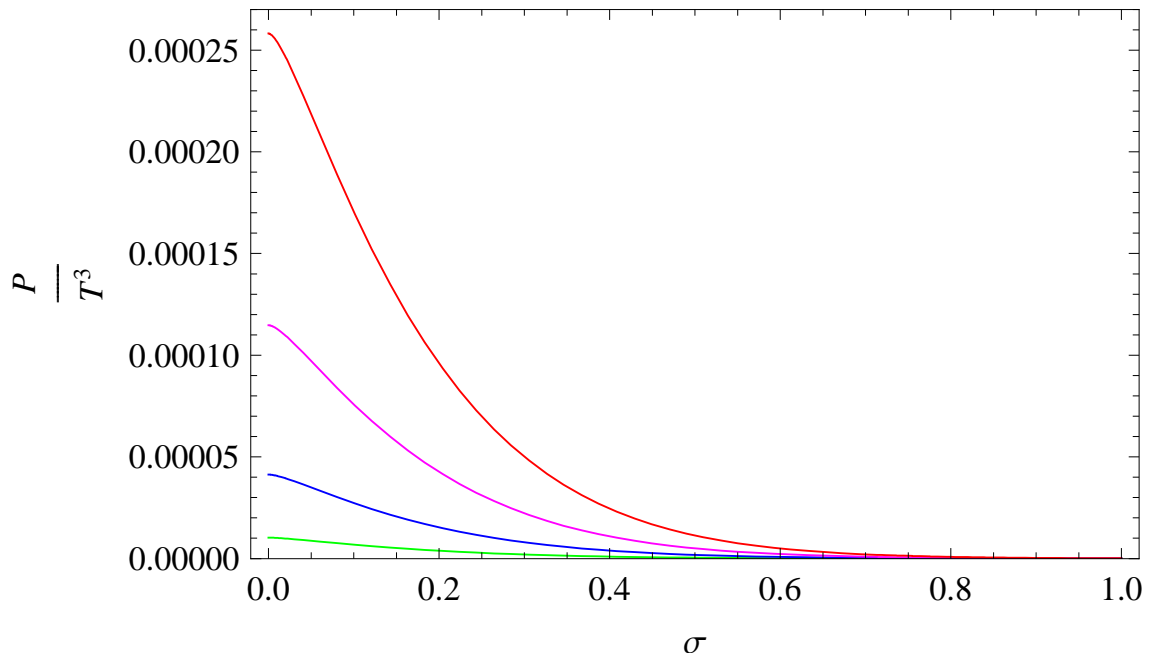


Figure 8: (2+1)-dimensional Heisenberg antiferromagnet: Three-loop interaction correction to the pressure as a function of the dimensionless ratio $\sigma = M_\pi/2\pi T$, evaluated at the same temperatures $T/F^2 = \{\frac{1}{10}, \frac{1}{5}, \frac{1}{3}, \frac{1}{2}\}T_{KT}/J$ as for the XY model in Fig. 4, from bottom to top in the figure.

5 D=2+1 Heisenberg Antiferromagnet at Low Temperatures

In this section we compare the results for the quantum XY model with the analogous results for the d=2+1 Heisenberg antiferromagnet within our three-loop analysis. Previous effective field theory studies of the d=2+1 Heisenberg antiferromagnet include Refs. [19, 20, 50–53].

Up to three-loop order, the pressure reads

$$P^{\text{AF}} = z_0^{\text{AF}} - z^{\text{AF}} = h_0(\sigma)T^3 - \frac{1}{F^4}q^{\text{AF}}(\sigma)T^5 + \mathcal{O}(T^6), \quad (5.1)$$

with z^{AF} given in Eq. (3.15). A plot for the function $q(\sigma)$, defined in Eq. (3.9), is provided for $N=3$ in Fig. 7. In the whole parameter regime σ , this function is negative. Accordingly, the spin-wave interaction in the pressure, much like for the d=2+1 quantum XY model, is always repulsive, as depicted in Fig. 8.

Interestingly, the spin-wave interaction gets stronger if the staggered field is weakened at fixed temperature – in contrast to the quantum XY model, where the strength of the interaction develops a maximum at $\sigma \approx 0.11$. Note that there is no two-loop contribution in the case of the Heisenberg antiferromagnet. Still, although we are

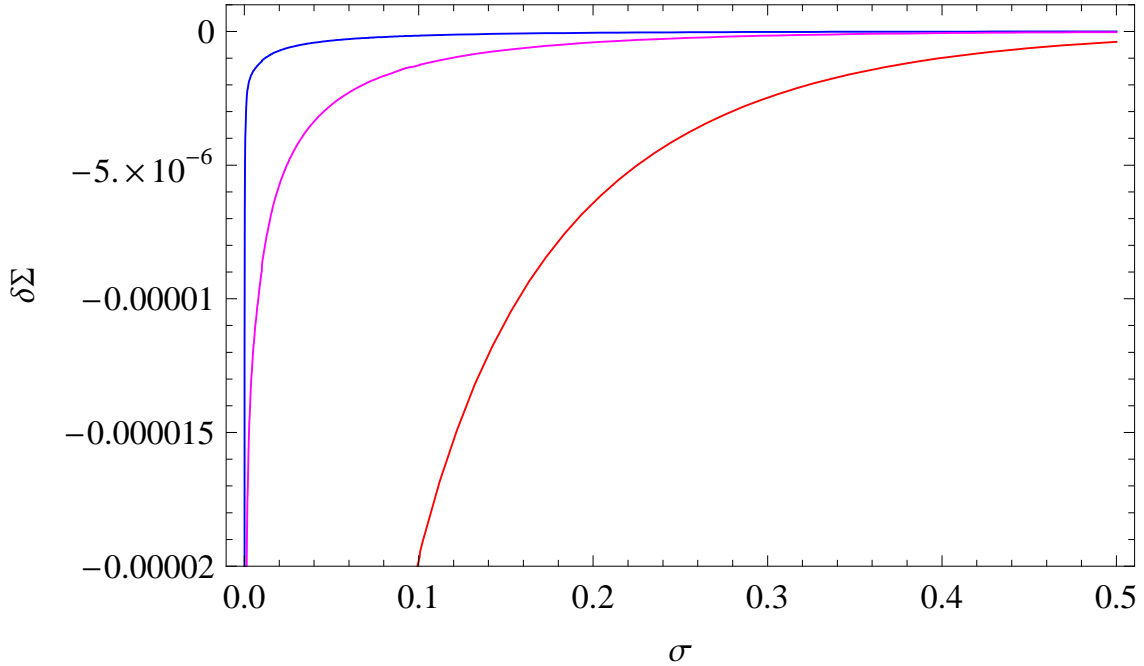


Figure 9: (2+1)-dimensional Heisenberg antiferromagnet: Temperature-dependent interaction correction to the staggered magnetization, $\delta\Sigma_s$, as a function of $\sigma = M_\pi/2\pi T$, evaluated at the same temperatures $T/F^2 = \{\frac{1}{10}, \frac{1}{5}, \frac{1}{2}\}T_{KT}/J$ as for the XY model in Fig. 6, from top to bottom in the figure. While the two-loop contribution is zero, the three-loop contribution is negative in the whole parameter region.

dealing with a three-loop effect, the strength P/T^3 of the spin-wave interaction is larger than in the quantum XY model for values of $T/F^2 \geq 0.24$ (compare Fig. 8 with Fig. 4). This is because (i) the coefficient of \bar{J}_1 in Eq. (3.9) is a factor of 24 smaller than the one of \bar{J}_2 and (ii) the quantity \bar{J}_1 is furthermore suppressed by four powers of σ , which is small in the relevant domain considered in the above plots.

In the temperature-dependent part of the staggered magnetization,

$$\delta\Sigma_s \equiv \frac{\Sigma_s^{\text{AF}}(T, H_s) - \Sigma_s^{\text{AF}}(0, H_s)}{\Sigma_s}, \quad \Sigma_s = \Sigma_s^{\text{AF}}(0, 0), \quad (5.2)$$

as can be seen in Fig. 9, the overall sign of the interaction correction is negative in the whole parameter range. Note that the spin-wave interaction only sets in at three-loop order. In the above plot we have used

$$\begin{aligned} \Sigma_s^{\text{AF}}(T, H_s) &= \Sigma_s^{\text{AF}}(0, H_s) - \frac{\Sigma_s b}{F^2} h_1(\sigma) T \\ &\quad - \frac{\Sigma_s b}{8\pi^2 F^6 \sigma} \frac{\partial q^{\text{AF}}(\sigma)}{\partial \sigma} T^3 + \mathcal{O}(T^4), \end{aligned} \quad (5.3)$$

along with the definition of b and $\Sigma_s^{\text{AF}}(0, H_s)$ given in Eqs. (4.4) and (4.5) for general N .

Formally, in the limit $\sigma \rightarrow 0$ (i.e., zero staggered field), the pressure reduces to

$$P^{\text{AF}} = \frac{\zeta(3)}{\pi} T^3 \left[1 - \frac{\pi q_1}{\zeta(3)} \frac{T^2}{F^4} + \mathcal{O}(T^3) \right], \quad (5.4)$$

where the coefficient $q_1 = q(\sigma = 0)$ is given by $q_1 = -0.008779$ (see Ref. [21]). In contrast to the quantum XY model, magnons related to the antiferromagnetic Heisenberg model keep interacting if the staggered external field is weakened. The corresponding expressions for u, s and c_V can be found in Eq. (5.7) of Ref. [21].

As for the XY model, the staggered magnetization of the Heisenberg antiferromagnet is logarithmically divergent in the limit $H_s \rightarrow 0$, due to the kinematical function $h_1(\sigma)$. Again, this divergence is purely mathematical, as it is forbidden to switch off completely the staggered field in our effective analysis. In the limit $H_s \rightarrow 0$, the "critical" temperature T_c , which marks the breakdown of the spin-wave picture, tends to zero.

But there is an important difference in the low-temperature dynamics of the quantum XY and the AF Heisenberg model in two spatial dimensions, we want to point out. Unlike the (2+1)-dimensional quantum XY model, the (2+1)-dimensional Heisenberg antiferromagnet develops a nonperturbatively generated mass gap at finite temperatures [54]. As outlined in detail in Ref. [21], this subtle effect also implies that the external field H_s cannot be switched off completely in our effective low-temperature expansions.

Yet another difference between the two models is the following. Although neither one of them exhibits spontaneously broken order at finite temperature and zero external field, the D=2+1 quantum XY model nonetheless has a finite transition temperature, while the D=2+1 antiferromagnetic Heisenberg model does not. One thus may raise the question whether this difference can be seen in the perturbative effective Lagrangian approach. The answer is negative, since the physics near the finite Kosterlitz-Thouless transition temperature of the D=2+1 quantum XY model occurring at $T_{KT} \approx 0.343J$ (square lattice), is beyond the reach of the effective Lagrangian method. The effective approach is only valid in the regime where the spin waves are the relevant degrees of freedom: low temperature and weak external field. The effective series are on safe grounds up to maybe one third of the topological transition temperature T_{KT} , but they definitely break down as one approaches T_{KT} from below. Hence the effective method cannot see this difference between the XY model and the antiferromagnet in two spatial dimensions.

6 Conclusions

Below the Kosterlitz-Thouless phase transition, which takes place at $T_{KT} \approx 0.343J$ for the square lattice, the physics of the d=2+1 quantum XY model is dominated by

the spin waves. Within the effective Lagrangian perspective, we have analyzed the partition function up to three loop-order and have derived the low-temperature series for various thermodynamic quantities, including the order parameter.

Although the low-temperature regime of the $d=2+1$ quantum XY model has been explored before, here, for the first time, to the best of our knowledge, we have performed a fully systematic study by using effective field theory. In particular, we have discussed how the spin-wave interaction manifests itself at low temperatures.

In the pressure, the interaction shows up at next-to-leading order through a term proportional to four powers of the temperature, related to a two-loop graph. Subsequent contributions originate from three-loop graphs and are of order T^5 . We also pointed out that, in the case of the $d=2+1$ Heisenberg antiferromagnet, the two-loop contribution is zero: the spin-wave interaction only sets in at order T^5 . Still, as we have explained, the strength of the interaction is larger in the Heisenberg antiferromagnet than in the quantum XY model. In both cases, the interaction is repulsive. While the spin-wave interaction in the $d=2+1$ quantum XY model tends to zero for very weak staggered field, in the $d=2+1$ Heisenberg antiferromagnet, on the other hand, the spin-wave interaction gets stronger.

It is essential that the external staggered field H_s in our effective analysis is kept finite. Switching it off completely, our effective series become meaningless, because the "critical" temperature T_c , below which the spin-wave picture is valid, tends to zero. This is how the Mermin-Wagner theorem raises its head in our effective calculation.

As we have argued, lattice anisotropies only become relevant in the subleading Lagrangian \mathcal{L}_{eff}^4 , giving rise to a next-to-next-to-leading order effect in the partition function, which does not affect our conclusions. Still, the lattice geometry does affect our results in a trivial way, because the low-energy constants Σ_s (staggered magnetization at zero temperature and zero external field), v (spin-wave velocity) and F^2 (spin stiffness or helicity modulus) take different values on e.g. the square and the honeycomb lattice.

We find it quite remarkable that all these results follow from symmetry considerations only. In particular, the fact that the spin-wave interaction in the pressure is repulsive, is an immediate consequence of the spontaneously broken symmetry $O(2)$ ($T = 0$) of the $d=2+1$ quantum XY model.

Acknowledgments

The author would like to thank C. J. Hamer, F. Niedermayer, J. Oitmaa and U.-J. Wiese for useful comments on the manuscript.

A Quantum XY Model versus Heisenberg Model

In this Appendix we point out that the effective descriptions of the quantum XY model and the Heisenberg model are different, although both systems are characterized by a spontaneously broken rotation symmetry at zero temperature. In particular, while there exists a mapping between the ferromagnetic and the antiferromagnetic quantum XY model also on the effective level, the Heisenberg ferromagnet is rather special.

On the microscopic level, the Heisenberg model,

$$\mathcal{H}_0 = -J \sum_{n.n.} \vec{S}_m \cdot \vec{S}_n, \quad (\text{A.1})$$

is invariant under internal spin $O(3)$ rotations. The ferromagnetic ($J > 0$) or antiferromagnetic ($J < 0$) ground states, however, are invariant only under $O(2)$. The well-known differences between ferromagnetic and antiferromagnetic spin waves – the former present a quadratic dispersion law, the latter follow a linear relation – have been analyzed from a unified perspective based on symmetries within the effective Lagrangian framework in Ref. [24]. The difference between the two systems can be traced back to the question whether or not the expectation value of the charge densities J_i^0 of the spin rotation symmetry is zero. The vacuum expectation value of J_i^0 is given by the spontaneous magnetization Σ ,

$$\langle 0 | J_i^0 | 0 \rangle = \delta_i^3 \Sigma, \quad i = 1, 2, 3, \quad (\text{A.2})$$

pointing here along the direction of the third axis. At leading order in the effective description of the ferromagnet, the spontaneous magnetization shows up as the coefficient of a topological term which involves only a single time derivative and dominates the low-energy properties of the system. More precisely, the leading-order effective Lagrangian of the Heisenberg ferromagnet takes the form (see Ref. [24])

$$\mathcal{L}_{eff}^2[F] = \Sigma \frac{\epsilon_{ab} \partial_0 U^a U^b}{1 + U^3} - \frac{1}{2} F^2 \partial_r U^i \partial_r U^i, \quad i = 1, 2, 3. \quad (\text{A.3})$$

It also contains a term with two spatial derivatives, proportional to the square of the low-energy constant F . Ferromagnetic spin-waves in the Heisenberg model thus obey a quadratic dispersion law.

On the other hand, since the spontaneous magnetization is zero for the Heisenberg antiferromagnet, the topological term with just one time derivative is absent. In the leading-order effective Lagrangian,

$$\mathcal{L}_{eff}^2[AF] = \frac{1}{2} F_1^2 \partial_0 U^i \partial_0 U^i - \frac{1}{2} F_2^2 \partial_r U^i \partial_r U^i, \quad i = 1, 2, 3, \quad (\text{A.4})$$

time and space derivatives are on the same footing. Antiferromagnetic spin waves follow a linear, i.e., relativistic dispersion law, with the velocity of light replaced by

the spin-wave velocity $v = F_2/F_1$. Setting $v \equiv 1$, we may use relativistic notation

$$\begin{aligned} \mathcal{L}_{eff}^2[AF] &= \frac{1}{2}F^2\partial_\mu U^i\partial^\mu U^i, \quad F_1 = F_2 = F, \\ & \quad i = 1, 2, 3, \end{aligned} \quad (\text{A.5})$$

where (pseudo-)Lorentz invariance is manifest. The essential point is to realize that the coefficient of the topological term, i.e. the spontaneous magnetization, makes the difference between Heisenberg ferromagnets and antiferromagnets on the effective level.

As pointed out in Ref. [24], the topological term can only arise when the spontaneously broken symmetry is non-Abelian. Therefore, despite the fact that the ferromagnetic XY model is also characterized by a nonzero spontaneous magnetization, the topological term is absent. At leading order in the effective description, there is thus no difference between the XY ferromagnet and the XY antiferromagnet. In either case the effective Lagrangian, using relativistic notation, is given by

$$\mathcal{L}_{eff}^2[XY] = \frac{1}{2}F^2\partial_\mu U^i\partial^\mu U^i, \quad i = 1, 2. \quad (\text{A.6})$$

This is equivalent to the statement that, in the absence of external fields, the ferromagnetic and antiferromagnetic quantum XY models can be mapped onto each other by a unitary transformation. Note that, apart from the number of magnon fields and the actual value of the low-energy coupling F , the effective Lagrangian for the quantum XY model (A.6) coincides with the effective Lagrangian (A.5) for the Heisenberg antiferromagnet.

We now consider the incorporation of external fields. On the microscopic level, in the Heisenberg model, one may introduce a magnetic field $\vec{H} = (0, 0, H)$ that couples to the magnetization vector $\sum_n \vec{S}_n$, and a staggered field $\vec{H}_s = (0, 0, H_s)$ that couples to the staggered magnetization vector $\sum_n (-1)^n \vec{S}_n$,

$$\mathcal{H} = \mathcal{H}_0 - \sum_n \vec{S}_n \cdot \vec{H} - \sum_n (-1)^n \vec{S}_n \cdot \vec{H}_s. \quad (\text{A.7})$$

Again we assume that the underlying lattice is bipartite. On the effective level, the leading-order Lagrangians for the ferromagnet and the antiferromagnet then take the form [25]:

$$\begin{aligned} \mathcal{L}_{eff}^2[F, H] &= \Sigma \frac{\epsilon_{ab}\partial_0 U^a U^b}{1 + U^3} - \frac{1}{2}F^2\partial_r U^i\partial_r U^i \\ & \quad + \Sigma H^i U^i, \quad i = 1, 2, 3, \end{aligned} \quad (\text{A.8})$$

$$\begin{aligned} \mathcal{L}_{eff}^2[AF, H_s, H] &= \frac{1}{2}F^2 D_\mu U^i D^\mu U^i + \Sigma_s H_s^i U^i, \\ & \quad i = 1, 2, 3. \end{aligned} \quad (\text{A.9})$$

As shown in Ref. [24], the magnetic field enters the effective Lagrangian $\mathcal{L}_{eff}^2[AF, H_s, H]$ in the time component of the covariant derivative of \vec{U} ,

$$D_0 U^i = \partial_0 U^i + \epsilon_{ijk} H^j U^k. \quad (\text{A.10})$$

Note that we do not consider the case where the staggered field is introduced for the ferromagnet.

At next-to-leading order, in the antiferromagnetic Lagrangian, the magnetic field \vec{H} shows up again in the covariant derivative D_0 ,

$$\mathcal{L}_{eff}^4[AF, H] = e_1(D_\mu U^i D^\mu U^i)^2 + e_2(D_\mu U^i D^\nu U^i)^2, \quad (\text{A.11})$$

where the quantities e_1 and e_2 are two additional low-energy constants. The ferromagnet, however, is rather special in the sense that the time derivatives, along with the magnetic field, can be eliminated with the equation of motion [30], such that the next-to-leading order Lagrangian takes the form

$$\begin{aligned} \mathcal{L}_{eff}^4[F, H] &= l_1(\partial_r U^i \partial_r U^i)^2 \\ &+ l_2(\partial_r U^i \partial_s U^i)^2 + l_3 \Delta U^i \Delta U^i. \end{aligned} \quad (\text{A.12})$$

Finally, the staggered field \vec{H}_s gives rise to the following three extra terms in the next-to-leading-order Lagrangian of the antiferromagnet [18]:

$$\begin{aligned} \mathcal{L}_{eff}^4[AF, H_s] &= k_1 \frac{\sum_s}{F^2} (H_s^i U^i) (\partial_\mu U^k \partial^\mu U^k) \\ &+ k_2 \frac{\sum_s^2}{F^4} (H_s^i U^i)^2 + k_3 \frac{\sum_s^2}{F^4} H_s^i H_s^i. \end{aligned} \quad (\text{A.13})$$

Gathering partial results, the effective Lagrangians up to order p^4 for the Heisenberg ferromagnet and antiferromagnet, in the presence of external fields, amount to

$$\begin{aligned} \mathcal{L}_{eff}^F[H] &= \Sigma \frac{\epsilon_{ab} \partial_0 U^a U^b}{1 + U^3} - \frac{1}{2} F^2 \partial_r U^i \partial_r U^i + \Sigma H^i U^i \\ &+ l_1 (\partial_r U^i \partial_r U^i)^2 + l_2 (\partial_r U^i \partial_s U^i)^2 \\ &+ l_3 \Delta U^i \Delta U^i, \quad i = 1, 2, 3, \end{aligned} \quad (\text{A.14})$$

and

$$\begin{aligned} \mathcal{L}_{eff}^{AF}[H, H_s] &= \frac{1}{2} F^2 D_\mu U^i D^\mu U^i + \Sigma_s H_s^i U^i \\ &+ e_1 (D_\mu U^i D^\mu U^i)^2 + e_2 (D_\mu U^i D^\nu U^i)^2 \\ &+ k_1 \frac{\sum_s}{F^2} (H_s^i U^i) (D_\mu U^k D^\mu U^k) + k_2 \frac{\sum_s^2}{F^4} (H_s^i U^i)^2 \\ &+ k_3 \frac{\sum_s^2}{F^4} H_s^i H_s^i, \quad i = 1, 2, 3. \end{aligned} \quad (\text{A.15})$$

We now turn to the quantum XY model. Interestingly, in the case of the Abelian symmetry $O(2)$, the term involving the magnetic field in the covariant derivative D_0

(A.10) vanishes. Hence the only field that matters for the XY antiferromagnet is the staggered field $\vec{H}_s = (0, H_s)$ and we have

$$\begin{aligned}
\mathcal{L}_{eff}^{XY,AF}[H_s] &= \frac{1}{2}F^2\partial_\mu U^i\partial^\mu U^i + \Sigma_s H_s^i U^i \\
&+ e_1(\partial_\mu U^i\partial^\mu U^i)^2 + e_2(\partial_\mu U^i\partial^\nu U^i)^2 \\
&+ k_1\frac{\Sigma_s}{F^2}(H_s^i U^i)(\partial_\mu U^k\partial^\mu U^k) \\
&+ k_2\frac{\Sigma_s^2}{F^4}(H_s^i U^i)^2 + k_3\frac{\Sigma_s^2}{F^4}H_s^i H_s^i, \\
&i = 1, 2.
\end{aligned} \tag{A.16}$$

In the case of the ferromagnet, again, the topological term involving just one time derivative can only occur if the spontaneously broken symmetry is non-Abelian. As a consequence, in the effective Lagrangian of the XY ferromagnet, unlike for the Heisenberg ferromagnet, time and space derivatives are on the same footing. The equation of motion no longer is of first order in the time derivative, such that time derivatives can no longer be eliminated. Finally, the magnetic field couples to the spontaneous magnetization vector \vec{U} , i.e., it enters the effective Lagrangian in the same way as the staggered field which couples to the staggered magnetization vector \vec{U} in the case of the XY antiferromagnet, namely

$$\begin{aligned}
\mathcal{L}_{eff}^{XY,F}[H] &= \frac{1}{2}F^2\partial_\mu U^i\partial^\mu U^i + \Sigma H^i U^i \\
&+ e_1(\partial_\mu U^i\partial^\mu U^i)^2 + e_2(\partial_\mu U^i\partial^\nu U^i)^2 \\
&+ k_1\frac{\Sigma}{F^2}(H^i U^i)(\partial_\mu U^k\partial^\mu U^k) + k_2\frac{\Sigma^2}{F^4}(H^i U^i)^2 \\
&+ k_3\frac{\Sigma^2}{F^4}H^i H^i, \quad i = 1, 2.
\end{aligned} \tag{A.17}$$

In conclusion, the systematic effective field theory analysis for the quantum XY model in the presence of magnetic and staggered fields just reflects what is known from the microscopic analysis. On a bipartite lattice, there is a one-to-one correspondence between the XY ferromagnet in a magnetic field, and the XY antiferromagnet in a staggered field.

B Cateye Graph in D=2+1: Evaluation

In the case of the antiferromagnetic Heisenberg model ($N=3$), the renormalization and subsequent numerical evaluation of the relevant integral J_2 ,

$$J_2 = \int_{\mathcal{T}} d^d x \left\{ \partial_\mu G(x) \partial_\mu G(x) \right\}^2, \tag{B.1}$$

was discussed in detail in Appendix A of Ref.[21]. The same techniques can be applied to the integral J_1 ,

$$J_1 = \int_{\mathcal{T}} d^d x \left\{ G(x) \right\}^4, \quad (\text{B.2})$$

which matters for the quantum XY model ($N=2$). This is the subject of the present Appendix. In either case, we are dealing with the evaluation of the cateye graph 5c of Fig. 1.

We first decompose the thermal propagator, defined in Eq. (3.12), into two pieces,

$$G(x) = \Delta(x) + \bar{G}(x), \quad (\text{B.3})$$

where $\Delta(x)$ is the zero-temperature propagator.

The singularities contained in J_1 can be removed by subtracting the following counterterms,

$$\bar{J}_1 = J_1 - c_1 - c_2 g_1(M, T), \quad (\text{B.4})$$

where $g_1(M, T)$ is the Bose function defined in Eq. (3.8). Using the method developed in Ref. [55], we now establish this result. This technique also allows us to derive expressions suitable for numerical evaluation.

The first step consists in cutting out a sphere \mathcal{S} around the origin of radius $|\mathcal{S}| \leq \beta/2$ and split the integral J_1 into two pieces,

$$J_1 = \int_{\mathcal{S}} d^d x \left\{ G(x) \right\}^4 + \int_{\mathcal{T} \setminus \mathcal{S}} d^d x \left\{ G(x) \right\}^4. \quad (\text{B.5})$$

The integrand in the second term, involving an integration over $\mathcal{T} \setminus \mathcal{S}$, is not singular, such that the limit $d \rightarrow 3$ poses no problems. In the first expression, where the integration extends over the sphere, we use the decomposition (B.3) and arrive at

$$\int_{\mathcal{S}} d^d x \left(\bar{G}^4 + 4\bar{G}^3 \Delta + 6\bar{G}^2 \Delta^2 + 4\bar{G} \Delta^3 + \Delta^4 \right). \quad (\text{B.6})$$

While the first three terms are convergent in $d=2+1$, the other two are divergent. The singularities contained therein can be taken care of as follows [55]. The quantity $\Delta(x)$ is Euclidean invariant. Therefore the expression

$$\int_{\mathcal{S}} d^d x 4\bar{G} \Delta^3 \quad (\text{B.7})$$

merely involves the angular average of $\bar{G}(x)$,

$$f(R) = \int d^{d-1} \Omega \bar{G}(x), \quad R = |x|. \quad (\text{B.8})$$

The function $\bar{G}(x)$ obeys the differential equation

$$\square \bar{G} = M^2 \bar{G}, \quad (\text{B.9})$$

which implies

$$\left(\frac{d^2}{dR^2} + \frac{d-1}{R} \frac{d}{dR} - M^2 \right) f = 0, \quad R < \beta. \quad (\text{B.10})$$

Now the function $g_1 ch(Mx_4)$ satisfies the same differential equation as $\bar{G}(x)$ and agrees with it at the origin. One thus concludes that the angular averages of the two quantities are identical:

$$\int_{\mathcal{S}} d^d x \bar{G} \Delta^3 = g_1 \int_{\mathcal{S}} d^d x ch(Mx_4) \Delta^3. \quad (\text{B.11})$$

Finally, decomposing the integral over the sphere according to

$$\begin{aligned} 4g_1 \int_{\mathcal{S}} d^d x ch(Mx_4) \Delta^3 &= 4g_1 \int_{\mathcal{R}} d^d x ch(Mx_4) \Delta^3 \\ &- 4g_1 \int_{\mathcal{R} \setminus \mathcal{S}} d^d x ch(Mx_4) \Delta^3, \end{aligned} \quad (\text{B.12})$$

the singularity now shows up in the integral over all Euclidean space,

$$c_2 = 4 \int_{\mathcal{R}} d^d x ch(Mx_4) \Delta^3. \quad (\text{B.13})$$

Turning to the last expression in Eq. (B.6), we remove the singularity by subtracting the temperature-independent integral of $\Delta(x)^4$ over \mathcal{R} ,

$$c_1 = \int_{\mathcal{R}} d^d x \Delta^4. \quad (\text{B.14})$$

Gathering partial results, the renormalized integral \bar{J}_1 in $d=2+1$ can be written as

$$\begin{aligned} \bar{J}_1 &= \int_{\mathcal{T}} d^3 x T + \int_{\mathcal{T} \setminus \mathcal{S}} d^3 x U - \int_{\mathcal{R} \setminus \mathcal{S}} d^3 x W, \\ T &= \bar{G}^4 + 4\bar{G}^3 \Delta + 6\bar{G}^2 \Delta^2, \\ U &= 4\bar{G} \Delta^3 + \Delta^4, \\ W &= 4g_1 ch(Mx_4) \Delta^3 + \Delta^4. \end{aligned} \quad (\text{B.15})$$

All pieces in the above representation of \bar{J}_1 are now finite. Since the quantities $\bar{G}(x)$ and $\Delta(x)$ only depend on $r = |\vec{x}|$ and on $t = x_4$, the above integrals are in fact two-dimensional

$$d^3 x = 2\pi r dr dt. \quad (\text{B.16})$$

Note that the size of the sphere, $|\mathcal{S}| \leq \beta/2$, introduced in the decomposition (B.5), is arbitrary and that the quantity \bar{J}_1 cannot depend on the specific radius of the sphere we choose. This fact allows us to check our numerical results. Indeed, we have verified that, using different sizes of the sphere, we arrive at the same result for the function $q(\sigma)$, which can be extracted from \bar{J}_1 through its definition (3.9).

References

- [1] M. Takahashi, Prog. Theor. Phys. Suppl. **87**, 233 (1986).
- [2] M. Takahashi, Phys. Rev. Lett. **58**, 168 (1987).
- [3] M. Kollar, I. Spremo and P. Kopietz, Phys. Rev. B **67**, 104427 (2003).
- [4] M. Uchinami, S. Takada and F. Takano, J. Phys. Soc. Jpn. **47**, 1047 (1979).
- [5] G. Gomez-Santos and J. D. Joannopoulos, Phys. Rev. B **36**, 8707 (1987).
- [6] C. J. Hamer, J. Oitmaa and Zheng Weihong, Phys. Rev. B **43**, 10789 (1991).
- [7] Zheng Weihong, J. Oitmaa and C. J. Hamer, Phys. Rev. B **44**, 11869 (1991).
- [8] L. Zhang, Phys. Rev. B **47**, 14364 (1993).
- [9] C. J. Hamer, T. Hövelborn and M. Bachhuber, J. Phys. A: Math. Gen. **32**, 51 (1999).
- [10] N. D. Mermin and H. Wagner, Phys. Rev. Lett. **17**, 1133 (1966).
- [11] K. Harada and N. Kawashima, J. Phys. Soc. Jpn. **67**, 2768 (1998).
- [12] H. De Raedt and B. De Raedt, Z. Phys. B - Condensed Matter **57**, 209 (1984).
- [13] H.-Q. Ding, Phys. Rev. B **45**, 230 (1992).
- [14] A. S. T. Pires, Phys. Rev. B **53**, 235 (1996).
- [15] A. W. Sandvik and C. J. Hamer, Phys. Rev. B **60**, 6588 (1999).
- [16] P. Tomczak and J. Richter, J. Phys. A: Math. Gen. **34**, L461 (2001).
- [17] C. Schindelin, H. Fehske, H. Büttner and D. Ihle, J. Magn. Magn. Mater. **226-230**, 403 (2001).
- [18] P. Hasenfratz and H. Leutwyler, Nucl. Phys. B **343**, 241 (1990).
- [19] P. Hasenfratz and F. Niedermayer, Phys. Lett. B **268**, 231 (1991).
- [20] P. Hasenfratz and F. Niedermayer, Z. Phys. B **92**, 91 (1993).
- [21] C. P. Hofmann, Phys. Rev. B **81**, 014416 (2010).
- [22] U. Gerber, C. P. Hofmann, F.-J. Jiang, M. Nyfeler and U.-J. Wiese, J. Stat. Mech. Theory Exp. (2009) P03021.
- [23] U. Gerber, C. P. Hofmann, F.-J. Jiang, G. Palma, P. Stebler and U.-J. Wiese, J. Stat. Mech. Theory Exp. (2011) P06002.

- [24] H. Leutwyler, Phys. Rev. D **49**, 3033 (1994).
- [25] C. P. Hofmann, Phys. Rev. B **60**, 388 (1999).
- [26] C. P. Hofmann, Phys. Rev. B **60**, 406 (1999).
- [27] J. M. Román and J. Soto, Int. J. Mod. Phys. B **13**, 755 (1999).
- [28] J. M. Román and J. Soto, Ann. Phys. **273**, 37 (1999).
- [29] J. M. Román and J. Soto, Phys. Rev. B **62**, 3300 (2000).
- [30] C. P. Hofmann, Phys. Rev. B **65**, 094430 (2002).
- [31] C. P. Hofmann, Phys. Rev. B **84**, 064414 (2011).
- [32] C. P. Hofmann, Phys. Rev. B **86**, 054409 (2012).
- [33] C. P. Hofmann, Phys. Rev. B **86**, 184409 (2012).
- [34] U. Gerber, C. P. Hofmann, F. Kämpfer and U.-J. Wiese, Phys. Rev. B **81**, 064414 (2010).
- [35] C. P. Hofmann, Phys. Rev. B **87**, 184420 (2013).
- [36] F. Kämpfer, M. Moser and U.-J. Wiese, Nucl. Phys. B **729**, 317 (2005).
- [37] C. Brügger, F. Kämpfer, M. Moser, M. Pepe and U.-J. Wiese, Phys. Rev. B **74**, 224432 (2006).
- [38] C. Brügger, F. Kämpfer, M. Pepe and U.-J. Wiese, Eur. Phys. J. B **53**, 433 (2006).
- [39] C. Brügger, C. P. Hofmann, F. Kämpfer, M. Pepe and U.-J. Wiese, Phys. Rev. B **75**, 014421 (2007).
- [40] C. Brügger, C. P. Hofmann, F. Kämpfer, M. Moser, M. Pepe and U.-J. Wiese, Phys. Rev. B **75**, 214405 (2007).
- [41] F.-J. Jiang, F. Kämpfer, C. P. Hofmann and U.-J. Wiese, Eur. Phys. J. B **69**, 473 (2009).
- [42] F. Kämpfer, B. Bessire, M. Wirz, C. P. Hofmann, F.-J. Jiang and U.-J. Wiese, Phys. Rev. B **85**, 075123 (2012).
- [43] N. D. Vlasii, C. P. Hofmann, F.-J. Jiang and U.-J. Wiese, Phys. Rev. B **86**, 155113 (2012).
- [44] T. Brauner, Symmetry **2**, 609 (2010).

- [45] C. P. Burgess, *Annu. Rev. Nucl. Part. Sci.* **57**, 329 (2007); *Phys. Rept.* **330**, 193 (2000).
- [46] J. L. Goity, *Czech. J. Phys.* **51**, B35 (2001).
- [47] S. Scherer, *Adv. Nucl. Phys.* **27**, 277 (2003).
- [48] H. Leutwyler, in *Hadron Physics 94 – Topics on the Structure and Interaction of Hadronic Systems*, edited by V. E. Herscovitz, C. A. Z. Vasconcellos and E. Ferreira (World Scientific, Singapore, 1995), p. 1.
- [49] G. Ecker, *Prog. Part. Nucl. Phys.* **35**, 1 (1995).
- [50] S. Chakravarty, B. I. Halperin and D. R. Nelson, *Phys. Rev. Lett.* **60**, 1057 (1988).
- [51] S. Chakravarty, B. I. Halperin and D. R. Nelson, *Phys. Rev. B* **39**, 2344 (1989).
- [52] H. Neuberger and T. Ziman, *Phys. Rev. B* **39**, 2608 (1989).
- [53] D. S. Fisher, *Phys. Rev. B* **39**, 11783 (1989).
- [54] P. Hasenfratz and F. Niedermayer, *Phys. Lett. B* **245**, 529 (1990).
- [55] P. Gerber and H. Leutwyler, *Nucl. Phys. B* **321**, 387 (1989).